

# Unsupervised SAR images change detection with hidden Markov chains on a sliding window

Zied Bouyahia<sup>1</sup>, Lamia Benyoussef<sup>2</sup> and Stéphane Derrode<sup>\*,2</sup>

\* Corresponding author

<sup>1</sup>École Nationale des Sciences de l'Informatique, Laboratoire CRISTAL,  
Campus Universitaire de la Manouba,  
2010 Manouba, Tunisia.

bouyahiazied@yahoo.fr

<sup>2</sup>Institut Fresnel (CNRS UMR 6133) & École Centrale Marseille,  
Technopôle de Château-Gombert, 38, rue Frédéric Joliot Curie,  
13451 Marseille Cedex 20, France.

{firstname.lastname}@ec-marseille.fr

## ABSTRACT

This work deals with unsupervised change detection in bi-date Synthetic Aperture Radar (SAR) images. Whatever the indicator of change used, *e.g.* log-ratio or Kullback-Leibler divergence, we have observed poor quality change maps for some events when using the Hidden Markov Chain (HMC) model we focus on in this work. The main reason comes from the stationary assumption involved in this model –and in most Markovian models such as Hidden Markov Random Fields–, which can not be justified in most observed scenes: changed areas are not necessarily stationary in the image. Besides the few non stationary Markov models proposed in the literature, the aim of this paper is to describe a pragmatic solution to tackle stationarity by using a sliding window strategy. In this algorithm, the criterion image is scanned pixel by pixel, and a classical HMC model is applied only on neighboring pixels. By moving the window through the image, the process is able to produce a change map which can better exhibit non stationary changes than the classical HMC applied directly on the whole criterion image. Special care is devoted to the estimation of the number of classes in each window, which can vary from one (no change) to three (positive change, negative change and no change) by using the corrected Akaike Information Criterion (AICc) suited to small samples. The quality assessment of the proposed approach is achieved with speckle-simulated images in which simulated changes is introduced. The windowed strategy is also evaluated with a pair of RADARSAT images bracketing the Nyiragongo volcano eruption event in January 2002. The available ground truth confirms the effectiveness of the proposed approach compared to a classical HMC-based strategy.

**Keywords:** Hidden Markov chain, Unsupervised classification, EM estimation, MPM classification, corrected Akaike Information Criterion, Change detection, SAR images.

## 1. INTRODUCTION

Bi-date change detection in SAR images is known to be a challenging task, mostly from the speckle inherent to this modality, and many algorithms have been proposed the last years. Among the post-classification comparison and the joint classification methods, the main approach used to detect changes between two date SAR images consists in segmenting a criterion image that exhibits change. Examples of such indicator of change are image difference, image ratio/log-ratio or Kullback-Leibler divergence.<sup>1-3</sup> For segmentation, among the numerous available supervised or automatic classification methods (SVM, genetic algorithms...), methods based on Markovian assumptions (Markov random fields,<sup>1,4,5</sup> Markov chains<sup>6,7</sup>) give encouraging results, for the same reasons that explain their nice SAR image segmentation performances:<sup>8</sup> the regularization effect of Markov models reduces the false detection rates consequently. However, for some observed scenes, Markovian models do not appear as efficient as expected to detect changes. The main reason comes from the stationary assumption involved in these

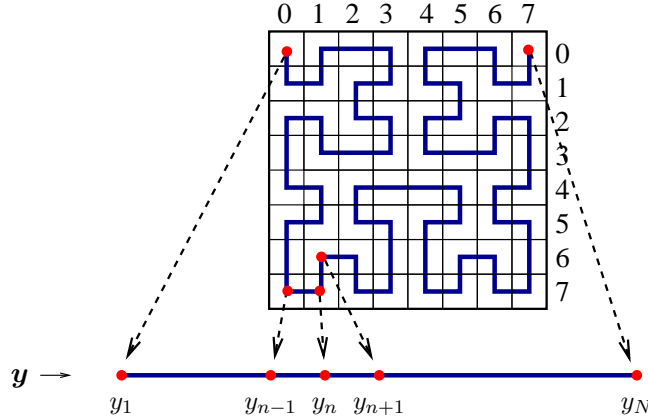


Figure 1. Hilbert-Peano scan construction for an  $8 \times 8$  image. This scan is used to transform a 2D image into a 1D signal, and conversely.

models, which can not be justified in most observed scenes: changed areas are not necessarily stationary in the image.

To overcome this problem and reduce the impact of stationarity on change detection results, we propose to segment the change indicator image with a Hidden Markov Chain (HMC) model<sup>9,10</sup> on a sliding window. In this algorithm, the criterion image is scanned pixel by pixel according to the Hilbert-Peano scan<sup>11</sup> (see Fig. 1). For each pixel  $n$ ,  $1 \leq n \leq N$  with  $N$  the total number of pixels in the image, we only consider a neighborhood of limited extend around it, *e.g.* 40 pixels before and 40 pixels after the pixel of interest ( $N_w = 81$ ). Classical HMC parameter estimation is then performed for each window  $W_n$  built that way using an Estimation-Maximization (EM) procedure under Gaussian assumption. Then, for the pixel  $n$  only, a Bayesian decision using the Marginal Posterior Mode (MPM) criterion is taken. By scanning entirely the criterion image (and using quick parameter update procedures to reduce computing time), the so-obtained change detection map is able to exhibit non stationary changes in the scene. This “windowed strategy” were motivated by a previous study<sup>12</sup> that shown the exponential decreasing influence of far-away pixels on so-called “forward” and “backward” probabilities used to estimate hidden parameters and to take MPM decision.<sup>13–15</sup> Special care is devoted to the estimation of the number of classes in each window, which can vary from one (no change) to three (positive change, negative change and no change) by using the corrected Akaike Information Criterion (AICc), which is known to be more robust than AIC and BIC (Bayesian Information Criterion) in case of small samples.<sup>16,17</sup>

The remaining of the paper is organized as follows: Section 2 recalls basic facts about unsupervised segmentation using the HMC model by means of an EM-based parameters estimation procedure and an MPM-based Bayesian classification. Section 3 explains how the HMC on a sliding window model can be used to reduce the impact of stationarity assumption of classical HMCs for unsupervised segmentation. Sections 4 and 5 present change maps obtained on synthetic and real radar data respectively, using log-ratio and Kullback-Leibler criteria as indicator of change.

## 2. UNSUPERVISED SEGMENTATION USING HMC

This section is intended to give some recalls about the HMC model<sup>15</sup> and its use for unsupervised image segmentation.<sup>9,10</sup> The HMC model can be adapted to a 2D analysis through a Hilbert-Peano scan of the image, see Fig. 1. Hence all estimation and segmentation processing are applied on the 1D sequence, and the segmented 2D image is reconstructed by using a reverse Hilbert-Peano scan from the 1D classified sequence.

**Model:** An image  $\mathbf{y} = \{y_1, \dots, y_N\}$ ,  $N$  being the total number of pixels, is considered as a realization of the 1D observed process  $\mathbf{Y} = \{Y_1, \dots, Y_N\}$ , each  $Y_n \in \mathbb{R}$ . The segmented image  $\mathbf{x} = \{x_1, \dots, x_N\}$  is considered as a realization of a hidden process  $\mathbf{X} = \{X_1, \dots, X_N\}$ , each  $X_n \in \Omega = \{1, \dots, K\}$ . In classical HMC,  $\mathbf{X}$  is assumed

to be a Markov chain, *i.e.*

$$p(x_{n+1} | x_n, \dots, x_1) = p(x_{n+1} | x_n).$$

The distribution of  $\mathbf{X}$  is consequently determined by the distribution of  $X_1$ , denoted by  $\pi_k = p(X_1 = k)$ , and the set of transition matrices  $(A^n)_{1 \leq n \leq N}$  whose elements are  $a_{ij}^n = p(X_{n+1} = j | X_n = i)$ . We further assume that  $\mathbf{X}$  is a stationary Markov chain, *i.e.* entries  $a_{ij}^n = a_{ij}$  do not depend on  $n$ . With the following additional properties

- Random variables  $Y_n$  are independent conditionally to  $\mathbf{X}$ :  $p(\mathbf{y} | \mathbf{x}) = \prod_{n=1}^N p(y_n | \mathbf{x})$ ,
- $p(y_n | \mathbf{x}) = p(y_n | x_n)$ ,

the distribution of the pairwise process  $(\mathbf{X}, \mathbf{Y})$  can be written as

$$p(\mathbf{x}, \mathbf{y}) = \pi_{x_1} f_{x_1}(y_1) \prod_{n=2}^N a_{x_{n-1}, x_n} f_{x_n}(y_n),$$

with  $f_{x_n}(y_n) = p(y_n | x_n)$  the data-driven densities, which are assumed to be Gaussian in this work (see Giordana *et al*<sup>10</sup> for generalized mixtures).

**Classification:** The estimation of  $\mathbf{X}$  from  $\mathbf{Y}$  can be realized by applying the MPM Bayesian criterion:

$$\forall n \in [1, \dots, N], \quad \hat{x}_n^{\text{MPM}}(\mathbf{y}) = \arg \max_{k \in \Omega} \xi_n(k), \quad (1)$$

with  $\xi_n(k) = p(X_n = k | \mathbf{y})$  the marginal *a posteriori* probabilities. The HMC model allows explicit computation of the MPM solution using the well-known Baum's "forward"  $\alpha_n(k)$  and "backward"  $\beta_n(k)$  probabilities,<sup>13</sup> modified by Devijver<sup>14</sup> for computational reasons:

$$\begin{aligned} \alpha_n(k) &= p(X_n = k | y_1, \dots, y_n), \\ \beta_n(k) &= \frac{p(y_{n+1}, \dots, y_N | X_n = k)}{p(y_{n+1}, \dots, y_N | y_1, \dots, y_n)}. \end{aligned}$$

Such probabilities can be computed recursively:

*Forward probabilities*

- Initialization: for  $n = 1$ ,

$$\forall k \in \Omega, \quad \alpha_1(k) = \frac{\pi_k f_k(y_1)}{\sum_{l \in \Omega} \pi_l f_l(y_1)}. \quad (2)$$

- Induction: for  $2 \leq n \leq N$ ,

$$\forall k \in \Omega, \quad \alpha_n(k) = \frac{f_k(y_n) \sum_{l \in \Omega} \alpha_{n-1}(l) a_{lk}}{\sum_{i \in \Omega} f_i(y_n) \sum_{l \in \Omega} \alpha_{n-1}(l) a_{li}}. \quad (3)$$

*Backward probabilities*

- Initialization: for  $n = N$ ,

$$\forall k \in \Omega, \quad \beta_N(k) = \frac{1}{K}. \quad (4)$$

---

**Algorithm 1** HMC parameters estimation using EM.
 

---

$q \leftarrow 0$ : Initialize parameters  $\theta^{[0]}$

**repeat**

-  $q \leftarrow q + 1$

- Compute “Forward”  $\alpha_n^{[q]}$  and “Backward”  $\beta_n^{[q]}$  probabilities using equations (2) to (5).

- Compute *a posteriori* probabilities  $\xi_n^{[q]}(k)$  using eq. (6) and  $\psi_n^{[q]}(k, l)$  using eq. (7).

- Estimate Markov chain parameters  $\theta^{[q]}$  using eq. (8) for Markov parameters and eq. (9) for Gaussian data-driven parameters.

**until**  $\|\theta^{[q]} - \theta^{[q-1]}\| < \text{Threshold}$ .

---

- Induction: for  $1 \leq n \leq N - 1$ ,

$$\forall k \in \Omega, \quad \beta_n(k) = \frac{\sum_{l \in \Omega} a_{kl} f_l(y_{n+1}) \beta_{n+1}(l)}{\sum_{i \in \Omega} f_i(y_{n+1}) \sum_{l \in \Omega} \alpha_n(l) a_{li}}. \quad (5)$$

It can be shown that marginal *a posteriori* probabilities can be written

$$\xi_n(k) = \alpha_n(k) \beta_n(k), \quad (6)$$

and joint *a posteriori* probabilities  $\psi_n(k, l) = p(X_n = k, X_{n+1} = l \mid \mathbf{y})$  as:

$$\psi_n(k, l) = \frac{\alpha_n(k) \beta_{n+1}(l) a_{kl} f_l(y_{n+1})}{\sum_{i \in \Omega} \sum_{j \in \Omega} \alpha_n(i) \beta_{n+1}(j) a_{ij} f_j(y_{n+1})}. \quad (7)$$

**Estimation:** Before classification, all parameters  $\theta = \{\pi_k, a_{kl}, f_k\}_{k, l \in \Omega}$  have to be estimated. One well-known solution is to use the EM iterative procedure<sup>18</sup> aiming at optimizing the log-likelihood of data, according to the steps described in Algorithm 1 above, with following update equations

$$\forall k \in \Omega, \quad \widehat{\pi}_k^{[q]} = \frac{1}{N} \sum_{n=1}^N \xi_n^{[q]}(k); \quad \forall k, l \in \Omega, \quad \widehat{a}_{kl}^{[q]} = \frac{\sum_{n=1}^{N-1} \Psi_n^{[q]}(k, l)}{\sum_{n=1}^{N-1} \xi_n^{[q]}(k)}. \quad (8)$$

$$\forall k \in \Omega, \quad \widehat{\mu}_k^{[q]} = \frac{\sum_{n=1}^N \xi_n^{[q]}(k) y_n}{\sum_{n=1}^N \xi_n^{[q]}(k)}; \quad \forall k \in \Omega, \quad \widehat{\sigma}_k^2^{[q]} = \frac{\sum_{n=1}^N \xi_n^{[q]}(k) (y_n - \widehat{\mu}_k^{[q]})^2}{\sum_{n=1}^N \xi_n^{[q]}(k)}. \quad (9)$$

### 3. HMC ON A SLIDING WINDOW

As mentioned above, unsupervised image segmentation using HMC is performed with the assumption that the Markov chain is stationary, which means that only one set of parameters  $\theta$  governed the whole segmented image. When the hidden chain is non stationary, the unsupervised restoration results using the HMC model can be poor, due to a bad match between the real and estimated models. Several methods have been proposed to break this limitation and some non stationary Markov model have been constructed by means of semi-Markov

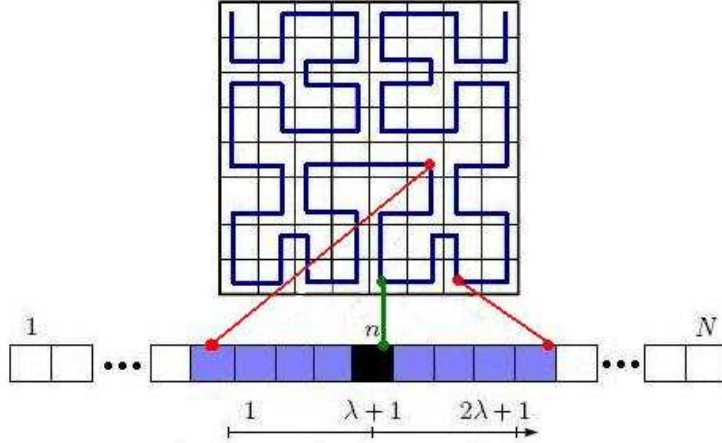


Figure 2. Principle of the HMC on a sliding window model.

chain or theory of evidence.<sup>19–23</sup> We propose here a simple and pragmatic algorithm to tackle the stationarity assumption, while preserving the regularization effect of Markovian models.

In this algorithm, the criterion image is scanned pixel by pixel according to the Hilbert-Peano scan.<sup>11</sup> For each pixel  $n$ ,  $1 \leq n \leq N$  with  $N$  the total number of pixels in the image, we only consider a neighborhood of limited extent around it, *e.g.* 40 pixels before and 40 pixels after the pixel of interest ( $\lambda = 40$ , and  $N_w = 2\lambda + 1 = 81$ ), see Fig. 2. HMC parameter estimation is then performed for each window  $W_n$  built that way using the EM procedure under Gaussian assumption, according to the procedure described in Section 2 and algorithm 1. Then, for the pixel  $n$  only, a Bayesian decision using the MPM criterion is taken.

By scanning entirely the criterion image, we estimate as many sets of parameters  $\theta$  as the number of windows, which is equal to the number of pixels  $N$ . Hence, while we consider a stationary Markov chain of limited extent centered on each pixel, the so-obtained segmented image is able to exhibit non stationary classes in the scene. From a computing resources point-of-view, the model can be used to segment very big images since the memory required for the model is limited to the memory necessary for an HMC with  $N_w \ll N$  pixels. To reduce computing time, we have implemented a quick parameters update procedure that initializes HMC parameters of one window from HMC parameters obtained at convergence from the previous window. Hence, only very few iterations are required for the EM to converge.

Using this windowed strategy, one difficulty arises for the estimation of the number of classes  $K_n$  in each  $W_n$ . Indeed, if the number of classes in the whole criterion image is known to be  $K = 3$ , corresponding to negative change, no change and positive change,  $K_n$  may vary between 1 and 3 and should be estimated in each window. This problem is known as “model or order selection” in the literature. Among information criteria available, we find BIC (Bayesian Information Criterion) and AIC (Akaike Information Criterion) which are given in the windowed context considered here by

$$\begin{aligned} BIC_{K_n} &= -2 \log L(\mathbf{y}; \hat{\theta}_{K_n}) + d_{K_n} \ln(N_w), \\ AIC_{K_n} &= -2 \log L(\mathbf{y}; \hat{\theta}_{K_n}) + 2 d_{K_n}, \end{aligned}$$

where

- $d_{K_n}$  denotes the number of free parameters of the model with order  $K_n$  ( $d_{K_n} = 3K_n - 1$ ),
- $\hat{\theta}_{K_n}$  the estimated parameters for the model of order  $K_n$ ,
- $L(\cdot)$  the likelihood function for the estimated model with parameter  $\theta_{K_n}$ .

Instead of these criteria, we used the corrected AIC criterion defined by

$$AICc_{K_n} = -2 \log L(\mathbf{y}; \hat{\theta}_{K_n}) + 2 \frac{N_w(d_{K_n} + 1)}{N_w - d_{K_n} - 2}, \quad (10)$$

which is known to be more robust than AIC and BIC in case of small samples.<sup>16,17</sup>

#### 4. UNSUPERVISED CHANGE DETECTION FROM SIMULATED SAR IMAGES

Ground-truth maps for real scenes are rarely available\*. A quantitative evaluation of change detection is then very difficult, especially for SAR images in which speckle makes things very more difficult than for optical/passive sensors. This is why we propose here to evaluate change detection accuracy of the HMC on a sliding window model for simulated SAR images in which synthetic changes have been introduced. Experimental results are conducted using the classical log-ratio detector and under Gaussian noise assumption.

##### 4.1 Speckle simulation and log-ratio criterion

Simulating SAR images is a very difficult task since ground reflectivity neither surface roughness are generally known. However, thanks to works by J. W. Goodman and under medium assumptions, it is possible to model the speckle statistically –the origin of which is inherent to coherent imaging systems/sensors like SAR ones– and to simulate somewhat realistic speckle images.

SAR images are produced by coherent summation of elementary scattered electromagnetic fields  $A \exp(j\phi)$ . Each pixel can be simulated by coherent summation of hundreds of reflectivity amplitude  $A_n$  and phases  $\phi_n$ :

- $A_n$  come from independent realizations of a Gamma distribution defined by a mean reflectivity value  $R$  and an heterogeneous coefficient  $\lambda = K R$ ,  $K$  being a proportionality coefficient between mean and variance of the multiplicative noise;
- $\phi_n$  come from independent uniform realizations in  $[0; 2\pi]$ .

Taking the square of the modulus of each pixel yields a one-look intensity image. Figure 3 presents the reference images of the scene before (a) and after (c) changes, and the introduced changes (b) between the two. Reference images are used as reflectivity maps to simulate speckle images (with  $K = 1.6$ ), as shown in Fig. 4.

The classical log-ratio detector is then applied on images 4(a) and (b) to emphasize changes, giving the criterion image (c), which is then segmented by using the HMC on a sliding window model. Log-ratio operator is the log-ratio of the mean value of pixels inside a fixed-size window

$$I_{LR}(i, j) = \log \left( \frac{\sum_{(k,l) \in N_{ij}} I_2(k, l)}{\sum_{(k,l) \in N_{ij}} I_1(k, l)} \right), \quad (11)$$

where  $N_{ij}$  denotes the neighboring pixels of the pixel  $(i, j)$  inside a boxed window<sup>†</sup>. This low-pass windowed filtering reduces the impact of speckle on the change map.

##### 4.2 Change detection results on simulated images

The first point to evaluate is the robustness of the estimation of classes number along the scan of the criterion image. Fig. 5 shows maps exhibiting the number of classes estimated in each window for two order-selection criteria cited above: BIC (b) and AICc (c). By comparing those maps with the true map (a), results obtained with AICc criterion are substantially better than those obtained with BIC criterion, confirming the good behavior of AICc in case of small samples.

---

\*one example is however given in Section 5.

<sup>†</sup>This window has nothing to do with the window invoked in the modified HMC model.

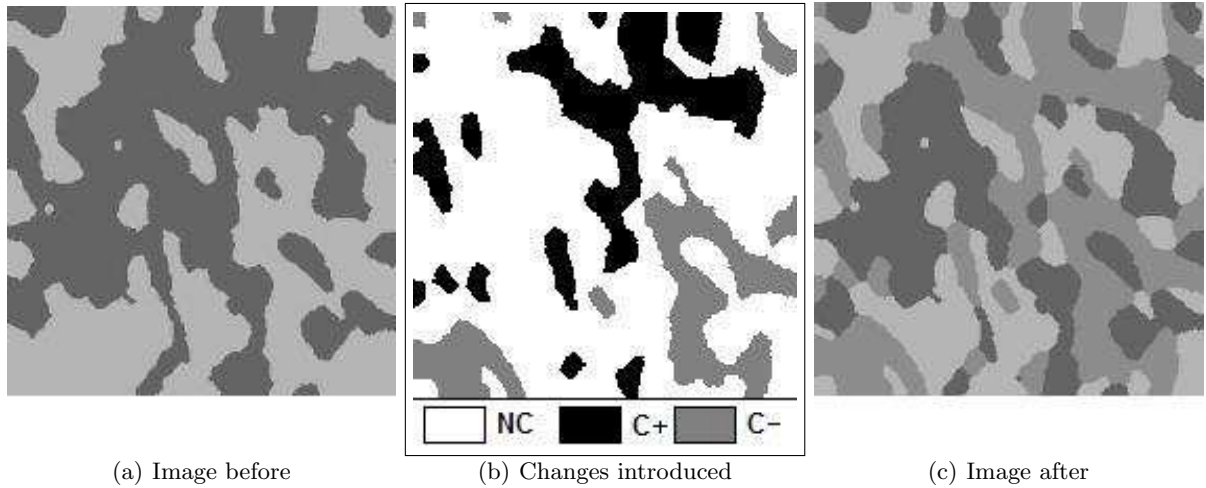


Figure 3. Reference images used to simulate bi-date SAR images for change detection (size  $128 \times 128$ ). In (b), NC means “no change”, C+ means “positive change” and C- means “negative change”.

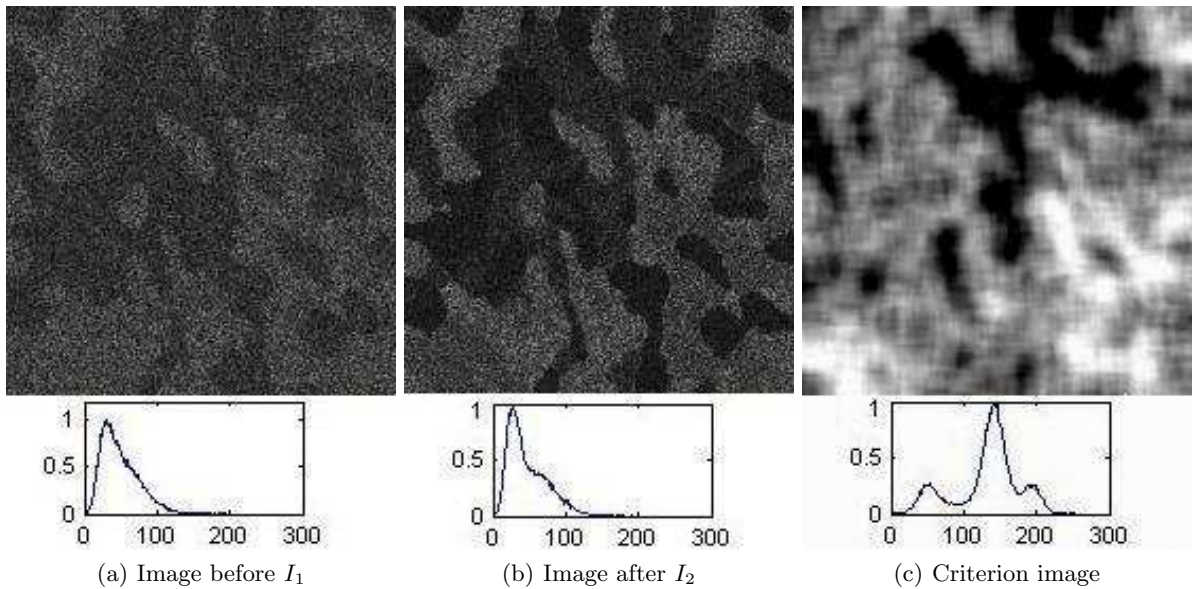


Figure 4. Simulated SAR images before (a) and after (b) changes, and corresponding criterion image (c) obtained from the log-ratio detector given in eq. (11).

Then the model has been evaluated for change detection. We performed the classification of the criterion image in Fig. 4(c) with  $K = 3$  classes corresponding to NC, C+ and C-, using classical HMC and HMC on a sliding window models. Fig. 6 presents the Receiver Operating Characteristics (ROC) curve, *i.e* the False Alarm Rate (FAR) according to the False Rejection Rate (FRR), for different window sizes. As expected, the change detection accuracy evolves with the size of the window. For this image, the optimal value of  $N_w$  is about 81 ( $\lambda = 40$ ), because it gives the best compromise between FAR and FRR. The FAR obtained with classical HMC model is almost three times bigger than  $HMC_{\lambda=40}$  one, whereas the FRRs are almost the same, producing a total error rate twice bigger for HMC than for  $HMC_{\lambda}$ . Segmentation results obtained with the classical HMC model and with the  $HMC_{\lambda=40}$  on a sliding window model are shown in Fig. 7.

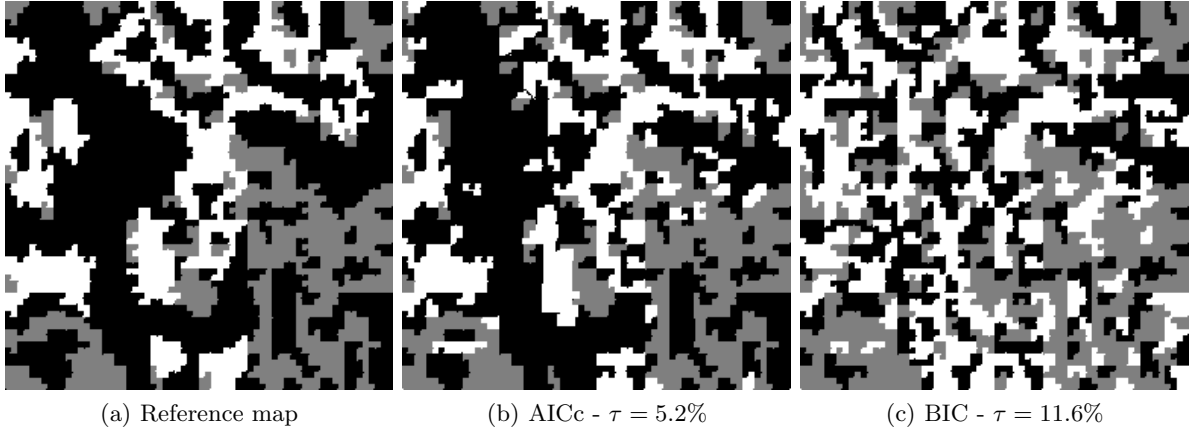


Figure 5. These maps show the number of classes estimated by AICc (b) and BIC (c) for  $N_w = 81$ , together with the optimal map computed from the original images in Fig. 3. Black, gray and white labels correspond respectively to 1, 2 and 3 classes.

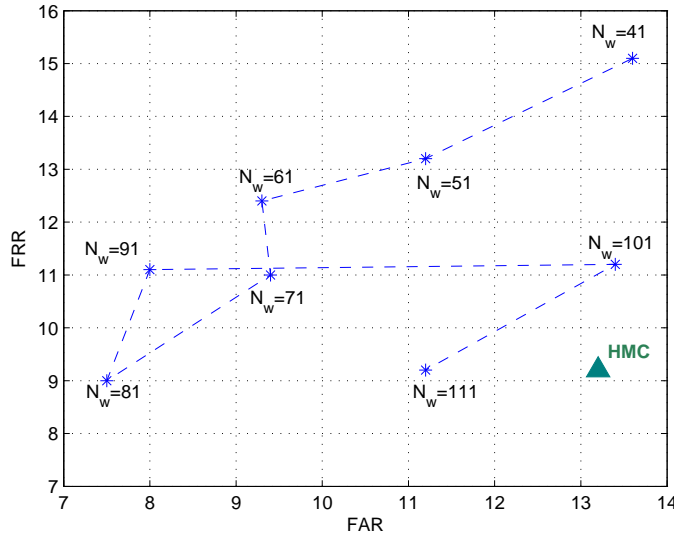


Figure 6. ROC curve obtained with the windowed HMC model under Gaussian distributions assumption according to  $N_w$ . The result obtained with the classical HMC model is point out by a triangle.

## 5. UNSUPERVISED CHANGE DETECTION IN SAR IMAGES

This section illustrates the application of the algorithm for the detection of lava pathes after the Nyiragongo eruption (Democratic Republic of Congo) event in January 2002. Fig. 8 shows two RADARSAT images acquired before and after the eruption. Both images have a ground resolution of  $10m$  covering an area of  $4Km$  in azimuth direction and  $8Km$  in range direction. Images were orthorectified by IGN-F (French National Geographic Institute) to a UTM35S projection, as for the ground-truth map shown in Fig. 8(c). Neither filtering nor calibration was applied. We follow on this scene the evolution of lava flow which arises from the summit of the volcano on top of the image and flows straight down to cover a part of a landing strip and ending in sea.

The detector used in this experience is the Kullback-Leibler distance, which is defined as the sum of the two

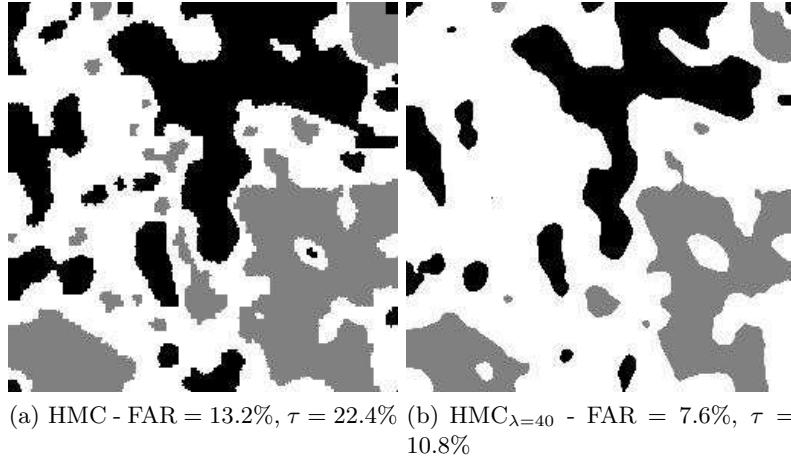


Figure 7. Change detection results without (a) and with (b) the windowed strategy. These maps have to be compared with Fig. 3(b).

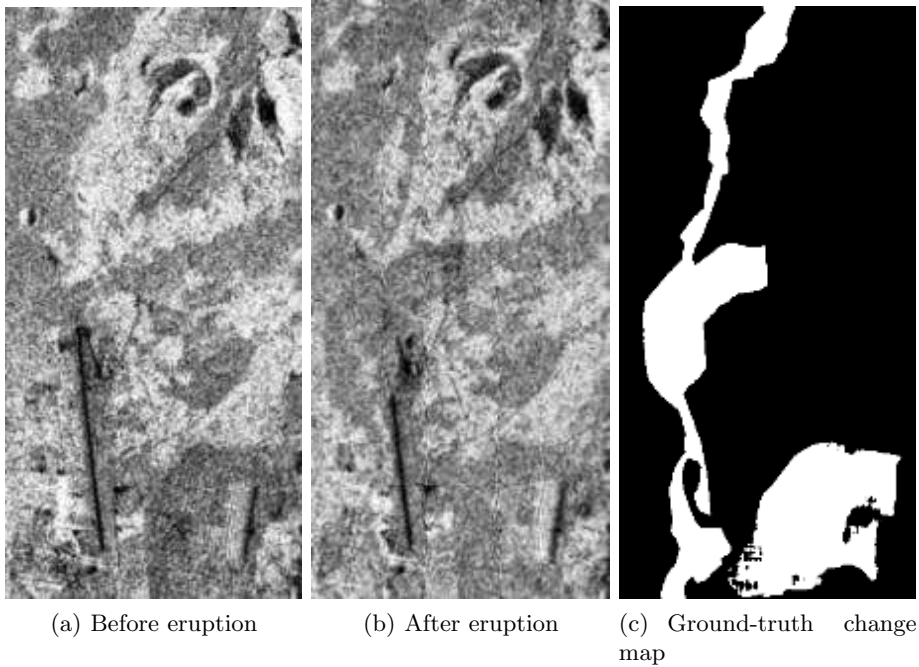


Figure 8. RADARSAT images of Nyiragongo volcano eruption in January 2002.

directed Kullback-Leibler divergence given by

$$\Delta_{KL}(p, q) = \int_{\mathbb{R}} \log \left( \frac{p(y)}{q(y)} \right) p(y) dy, \quad (12)$$

for  $p$  and  $q$  two probability density functions defined on  $\mathbb{R}$ . Fig. 9(a) presents the criterion image so obtained.

Change maps in Fig. 9 show the classification results of the criterion image into two classes: change and no change. False alarm rates, computed by comparison of the change map with the mask, see Fig. 8(c), confirm that HMC on sliding window provides really better change detection results than the classical HMC model. The error rates confirm the nice overall performance of our algorithm.

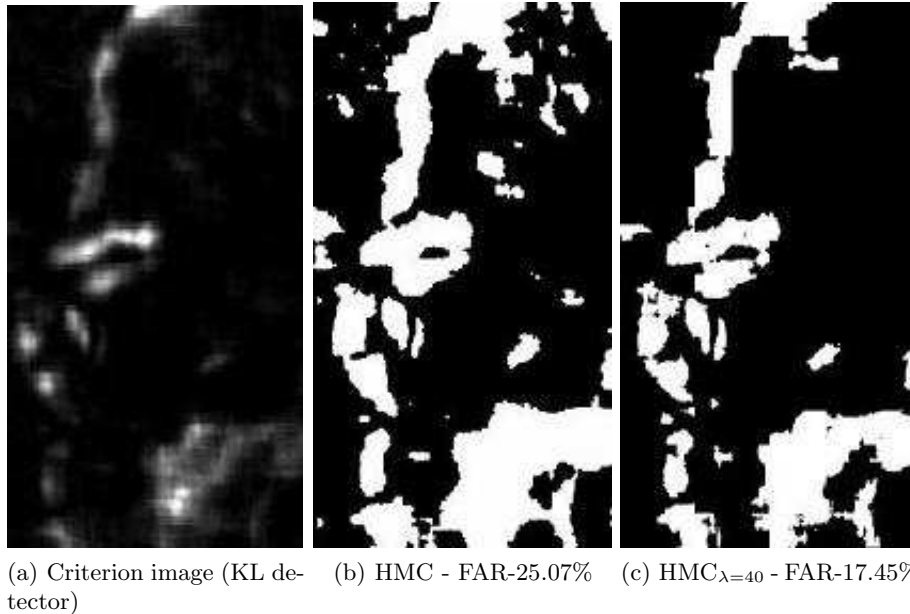


Figure 9. Change maps obtained using classical HMC model (b) and HMC on a sliding window of size  $\lambda = 40$  (c).

## 6. CONCLUSION

In this paper, we focused on SAR image change detection which is a challenging application of remote sensing. To detect changes we perform a classification of a so-called criterion image obtained with a detector such as the log-ratio or Kullback-Leibler distance. The segmentation of the criterion image by HMC can be inappropriate due to the stationary assumption the model relies on. To overcome this problem we proposed an extension of the classical HMC model to be used on a sliding window, which allows to take into account non-stationarities in images.

Comparison of change detection results on simulated and real SAR images shows that the proposed extension improves change detection robustness compared to a classical HMC classification, whatever the change criterion used. Additionally, the windowed strategy allows to treat images of any size while the classical HMC model is limited by heavy computer memory requirements. The question of the optimal size for the window is still an open issue and should depend on the image content.

## REFERENCES

1. L. Bruzzone and D. F. Prieto, "Automatic analysis of the difference image for unsupervised change detection," *IEEE Transactions on Geoscience and Remote Sensing* **38**(3), pp. 1171–1182, 2000.
2. E. J. M. Rignot and J. J. V. Zyl, "Change detection techniques for ERS-1 SAR data," *IEEE Transactions on Geoscience and Remote Sensing* **31**(4), pp. 896–906, 1993.
3. J. Inglada and G. Mercier, "A new statistical similarity measure for change detection in multitemporal SAR images and its extension to multiscale change analysis," *IEEE Transactions on Geoscience and Remote Sensing* **19**(5), pp. 465–475, 2007.
4. T. Kasetkasem and P. K. Varshney, "An image change detection algorithm based on Markov random field models," *IEEE Transactions on Geoscience and Remote Sensing* **40**(8), pp. 1815–1823, 2002.
5. F. Melgani and Y. Bazi, "Robust unsupervised change detection with Markov random fields," in *IEEE Int. Geoscience and Remote Sensing Symp. (IGARSS'06)*, (Denver, Colorado, USA), July 31 - August 4 2006.
6. S. Derrode, G. Mercier, and W. Pieczynski, "Unsupervised change detection in SAR images using a multi-component HMC model," in *MultiTemp'03*, (Ispira, Italy), 16-18 July 2003.

7. C. Carincotte, S. Derrode, and S. Bourennane, "Unsupervised change detection on SAR images using fuzzy hidden Markov chains," *IEEE Transactions on Geoscience and Remote Sensing* **44**(2), pp. 432–441, 2006.
8. R. Fjørtoft, Y. Delignon, W. Pieczynski, M. Sigelle, and F. Tupin, "Unsupervised segmentation of radar images using HMC and HMRF," *IEEE Transactions on Geoscience and Remote Sensing* **41**(3), pp. 675–686, 2003.
9. B. Benmiloud and W. Pieczynski, "Estimation des paramètres dans les chaînes de Markov cachées et segmentation d'images," *Traitement du Signal* **12**(5), pp. 433–454, 1995.
10. N. Giordana and W. Pieczynski, "Estimation of generalized multisensor hidden markov chains and unsupervised image segmentation," *IEEE Transactions on Pattern Analysis and Machine Intelligence* **19**(5), pp. 465–475, 1997.
11. W. Skarbek, "Generalized Hilbert scan in image printing," in *Theoretical Foundations of Computer Vision*, Akademik Verlag, Berlin, 1992.
12. S. Derrode, L. Benyoussef, and W. Pieczynski, "Contextual estimation of hidden Markov chains with application to image segmentation," in *IEEE Int. Conf. on Acoustics, Speech, and Signal Processing (ICASSP'06)*, (Toulouse, France), 14-19 May 2006.
13. L. Baum, T. Petrie, G. Soules, and N. Weiss, "A maximization technique occurring in the statistical analysis of probabilistic functions of Markov chains," *The Annals of Mathematical Statistics* **41**(1), pp. 164–171, 1970.
14. P.-A. Devijver, "Baum's Forward-Backward algorithm revisited," *Pattern Recognition Letters* **3**, pp. 369–373, 1985.
15. L. R. Rabiner, "A tutorial on HMMs and selected applications in speech recognition," *Proc. of IEEE* **77**(2), pp. 257–286, 1989.
16. N. Sugiura, "Further analysis of the data by Akaike's information criterion and the finite corrections," *Communications in Statistics. Theory and Methods* **7**(1), pp. 13–26, 1978.
17. C. M. Hurvich and C.-L. Tsai, "Regression and time series model selection in small samples," *Biometrika* **76**(2), pp. 297–307, 1989.
18. A. P. Dempster, N. M. Laird, and D. B. Rubin, "Maximum likelihood from incomplete data via the EM algorithm," *Journal of the Royal Statistical Society* **39**(1), pp. 1–38, 1977.
19. B. Sin and J. H. Kim, "Nonstationary hidden Markov model," *Signal Processing* **46**, pp. 31–46, 1995.
20. P. M. Djuric and J. H. Chun, "An MCMC sampling approach to estimation of nonstationary hidden Markov models," *IEEE Transactions on Signal Processing* **50**(5), pp. 1113–1123, 2002.
21. S.-Z. You and H. Kobayashi, "A hidden semi-Markov model with missing data and multiple observation sequences for mobility tracking," *Signal Processing* **83**, pp. 235–250, 2003.
22. P. Lanchantin and W. Pieczynski, "Unsupervised restoration of hidden non stationary Markov chain using evidential priors," *IEEE Transactions on Signal Processing* **53**(8), pp. 3091–3098, 2005.
23. D. Benboudjema and W. Pieczynski, "Unsupervised statistical segmentation of non stationary images using triplet Markov fields," *IEEE Transactions on Pattern Analysis and Machine Intelligence* **29**(8), pp. 1367–1378, 2007.